Proceedings of the
International Conference on Mechanical Engineering and Renewable Energy 2011
(ICMERE2011) 22- 24 December 2011, Chittagong, Bangladesh

ICMERE2011-PI-188

FEASIBILITY OF STATIC COMPUTATIONAL FLUID DYNAMICS SIMULATIONS AROUND A SPECIALISED DELTA WING CONFIGURATION

Christopher Pevitt*, **Rachel Ong and Firoz Alam**

School of Aerospace, Mechanical and Manufacturing Engineering, RMIT University, Melbourne, Australia
*E-mail: christopher.pevitt@student.rmit.edu.au

Abstract- *The goal of this paper was to determine if it was feasible to accurately model the full static angle of attack range in Computational Fluid Dynamics (CFD) applications while determining associated model dependencies. If successful, this would be a step towards CFD being utilised as a more reliable tool in the development of aircraft. This process could reduce the reliance on wind tunnel results with a consequent reduction in development costs. The test bed used for this paper was based on a specialised delta wing configuration. The study was undertaken by comparing simulation parameters such as mesh resolution, Discretisation schemes, turbulence and transition models, time step sizes and the order of the time integration operator. The analysis was completed using specialised meshing software, the flow simulation software (TAU) developed by the German Aerospace Agency (DLR) and the graphical interface Tecplot. Findings indicated that the capabilities to accurately model the flight envelope of the configuration are available but are also limited. Results showed the difficulties in utilising one CFD model to represent the entire angle of attack range and the large effects model dependencies can have on results.*

Keywords: Computational Fluid Dynamics (CFD), Delta Wing, Tecplot, TAU, Stability and Control, Dynamic

1. INTRODUCTION

Computational Fluid Dynamics (CFD) simulations have been used to a significant extent in the development of aircraft. As software capabilities and computing power have increased over time, the importance of and reliance upon, CFD simulations has similarly increased. The simulation results have progressively become more accurate and reliable. However the data provided by CFD simulations has had limitations. As such, the results of CFD simulations have never been relied on as the sole source of data. The results were always validated with additional testing, either via wind tunnel testing or flight tests, both of which are costly and time consuming. Also, these options were not always practical or suitable alternatives. Additionally, under certain flight characteristics the wind tunnel results did not entirely represent the true flow over the aircraft.

It is preferable if all flight characteristics are known before the full scale aircraft enters flight testing. Once full scale flight testing commences, it is very costly to make changes to the aircraft. Furthermore, unexpected aircraft handling during testing can be very dangerous. Therefore, it would be greatly beneficial to improve the reliability and accuracy of CFD simulations which would reduce the necessity for additional alternative testing. This would help to reduces costs in addition to opening up possibilities for more detailed testing under the entire flight envelope of the aircraft.

With recent advances in the Aerospace industry, the demand and commonality of Unmanned Aerial Vehicles (UAV) has increased. These planforms often lead to configuration with nonlinear aerodynamic behaviour; this can be dominated by vortical flow across the upper surfaces. Many of the characteristics of flow phenomena associated with highly swept delta wings have been well documented [1]. However, the flow is not entirely understood in less swept wings with rounded leading edges. It is these characteristics that need to be better understood in order to effectively enhance future developments of aircraft and the use of CFD.

The determination of static flow characteristics in aircraft development is an essential part of the development cycle in flight physics. When reviewing an unstable aircraft, knowledge of the flight characteristics are critical for design of the flight control systems. This is vital, as many future unmanned aircraft configurations exhibit aerodynamic stability and control issues in various regions of their flight envelope.

The goal of this paper is to determine the feasibility of static CFD simulation around the specialised delta wing in the interesting AoA (Angle of Attack) range. During this process individual parameters will be assessed. These include the dependencies on configurations (with and without sting), mesh resolutions, discretisation schemes, turbulence and transition models, time step sizes and order of the time integration

© ICMERE2011

operations. The results of these tests will then be compared to the characteristics of both in-phase and out-of phase contributions to the global forces and moments.

2. AERODYNAMICS OF DELTA WINGS

The Delta wing is a common design utilised in the development of supersonic aircrafts around the world [2]. There are a large number of delta wing types including; Standard, Ogival, Compound, Cropped, Tailless, Cranked Arrow and Diamond/Lambda configurations [3]. These configurations can be seen in Figure 1.

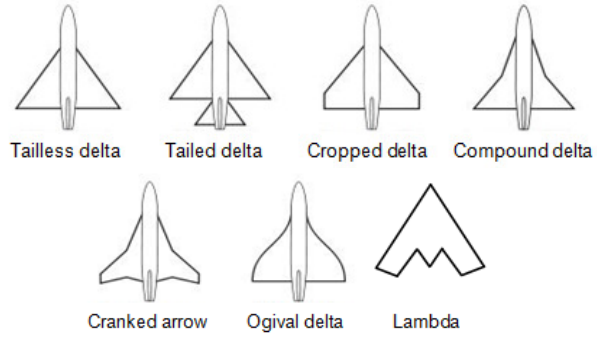

Fig.1: Delta Wing Configurations [3]

The delta wing configuration that is used for this paper is a Lambda type of delta wing with a 53º swept wing. In addition to the delta configuration, that sweep angle of the wings also characterizes the type of delta wing, between slender and non-slender. A non-slender delta wing is defined as having a sweep angle equal or less than 55º [1]. These are known as low sweep angle wings. This means the configuration used is also characterised as a low sweep angle, non-slender, lambda delta wing.

A method of characterising a slender delta wing is through its sweep angle. This consists of wings with a sweep angle equal or greater than 65º. The majority of testing that has been performed to date has been focused on slender delta wings. Due to this many aerodynamic investigations, examining the flow physics around this this type of configuration, have been conducted. As a result the flow phenomenon that is seen is quite well understood [4]. This type of configuration is often this is seen in modern day Jet fighters.

A non-slender delta wing is denoted as a delta wing with a sweep angle equal or less than 55º. Initial findings in computations and experimental studies revealed that at low AoA non-slender delta wings will form a “dual” primary vortex structure over the configuration [1]. Based on the work done by Gursul, it is noted that “this particular vortex structure is a result of the proximity of the vortex formation to the wing surface, and the corresponding interaction with the surface boundary layer”. Other findings have come to the conclusion that this formation is unique to non-slender delta wings.

Another key feature of the non-slender delta wing is that the flow separation and the formation of the vortices will occur at very low AoA. The complete vortex development will not develop until higher AoA. As the vortical flow forms over the wing surface, the vortices will interact with the boundary layer. This will result in the formation of a dual vortex system [1].

Advantages of this type of delta wing are the possibility of reduced drag capabilities. This could lead to better performance and flight characteristics for long range and endurance aircraft [5]. The Delta wing configuration that was looked at in detail for the work in this paper was a non-slender delta wing. This was selected due to its complex flow characteristics and not well understood flow phenomena

Prior studies have illustrated that slender delta wings are capable of producing high lift and maneuverability capabilities due to their vortex structure. These same properties are not evident with non-slender delta wings; where a lower maximum lift coefficient and lower stall angle will be seen. It has been noted that the lift contributions become a smaller proportion of the total lift over the wing with decreasing sweep angles. Due to this there is no obvious correlation between the onset point of vortex breakdown and the changes in the lift coefficient [1].

Delta wings configurations have a low wing-per-unit loading capability allowing for improved manoeuvrability. This is possible as the delta configuration provides a larger total wing area than a standard configuration; which is useful for lift over the wing shape used [1]. Additionally delta wings have the ability of having higher stalling angles then standard wing configurations. This is due to the vortex generation capabilities of this planform. As the AoA increases, the leading edge of the aircraft will form larger vortices, which energises the flow, delaying the flow separation point and delaying stall [1].

Another advantage of the delta wing is its additional low speed capabilities. A standard configuration aircraft that is built to be optimum at high speeds will then be particularly unstable and dangerous at low speeds. This effect is a disadvantage for low speed manoeuvrers, especially landing. Additionally the non-slender delta wing configuration will be capable of flying efficiently at higher speeds, while remaining stable at lower speeds. This is due to the vortex generation process over the wing at higher speeds [1].

3. MODEL CONFIGURATION

The model is a specifically designed UCAV (Unmanned Combat Air Vehicle) delta wing configuration. It was developed for research purposes as part of the NATO (North Atlantic Treaty Organization), RTO (Research Technology Organisation) task group. The model has been specifically designed in order to develop key aerodynamic characteristics such as flow separation and the development of vortices. The exact configuration used can’t be shown due to current confidentially restrictions. The model has a 52º swept leading edge with the capability of interchanging a sharp or rounded leading edge. For this paper, the rounded leading edge will be used. The rounded leading edge configuration is created with a sharp inboard leading edge which transitions into a medium round leading edge on the outer panels of the wing. The outer panel has a parallel leading and trailing edge with a washout twist of 5º [6].

The model consists of three main sections; the

© ICMERE2011

fuselage, the wing section and wing tips. It is made of a light weight reinforced plastic that brings its overall weight to less than 10 kg [7]. The purpose of the extra light model is that it reduces the dynamic inertial loads. This allows for a more accurate and sensitive balance, which leads to better force and moment resolution. The model consists of more than 200 pressure taps on the upper and lower side of the model which are set to determine the dynamic measurements of unsteady pressure. The model was designed to gather both static and dynamic results.

4. COMPUTATIONAL PROCEDURE

The CFD simulation software that was used in this work was the DLR TAU-Code. This is a software package developed by the DLR Institute of Aerodynamics and Flow Technology. It was designed to be capable of solving complex CFD simulations. The solver is based around the compressible three-dimensional, steady, and unsteady Reynolds Averaged Navier-Stokes equations [8]. For this work, an unstructured grid will be used that is developed with an in-house meshing program called "Mesher". The TAU-Code has the capabilities to utilise both the Cell-Vertex and the Cell-Centered schemes, both with their own advantages and disadvantages. For this paper, the Cell-Centered scheme was used. In the Cell-Centered approach, the Navier-Stokes equations are solved on a dual background grid, which is determined directly from the primary grid [9]. This approach was used as it consists of a larger number of solution variables than other approaches, which would in turn lead to greater accuracy. The TAU-Code is capable of performing many different tasks and these can be split into five main modules. These modules can be seen as [8]:

a) Preprocessor – Takes information from the Primary grid to develop a dual-grid or multi-grids.

b) Solver – Performs the flow calculations over the dual-grid.

c) Adaption – Refines and de-refines the grid to allow for the capture of all flow phenomena. This includes a large range of categories, including the representation of vortex structures and shear layers around viscous boundaries.

d) Deformation – Propagates the deformation of surface-coordinates to the surround grid.

e) Motion – Defines the motion of the model and relates this motion to any control devices.

Many of these modules are inbuilt within the code and for this paper; they will not be altered from their default values. As a result, the Preprocessor and Solver modules will be examined in more detail while the other modules will be taken as non-variable.

The Preprocessor module is based on the meshed grid forming the primary grid. For this paper, a system of five dual grids was used. This introduction of multiple grids greatly improves the computational time and power required to run any simulation.

The Solver module calculates the gradients in time, which are then discretised through the use of a multi-step Runge-Kutta scheme. These calculations are then calculated using multigrid techniques and local time stepping which accelerates the ability to find converged results for steady state solutions [9].

5. NUMERICAL RESULTS

5.1 Initial CFD Findings

In order to determine the possible accuracy of CFD simulations and how different parameters can be improved the quality of the results initial simulations needed to be made. To be able to check these parameters accurately it was first important to ensure a good quality grid density. The mesh created can dramatically affect the results of the simulation. Due to this it is important to perform a mesh convergence study. As all models are different there are no hard and fast rules to mesh generation, the goal is to find a good quality mesh capable of capturing all key features of the flow. Originally three different meshes were created in the mesh generation process. Then based on initial simulation results a fourth model was developed. To explain the justification of the fourth model and to compare the effect of mesh refinement, the force and moment results for all three of the initial meshes were reviewed. Due to constraints in this paper only the pitching moment results will be shown. The first three meshed that were looked at had 1.5, 9.6 and 10.5 million nodes.

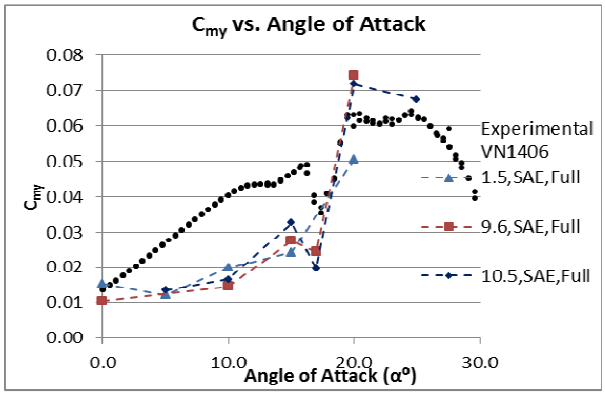

Fig. 2: Test VN 1406, SAE – 1.5, 9.6, 10.5 results C_{my} vs. Angle of Attack

When looking at the force and moment data for C_L and C_D, it was seen that all of the meshes could represent the experimental flow characteristics. While in Figure 2 for the pitching coefficient (C_{my}) it was seen that there are large variations between the CFD simulations and the experimental data. It was also noted that the variations increased for courser models as the AoA of the model increases. Though as the variations in the results are less for the two higher meshes, this indicates that the model is moving towards a mesh converged state. To try and explain the reasons for this

To further understand why there is a difference in the results of each of the meshes the surface contours were taken of the pressure coefficient over the configuration. These comparisons can be seen visually for an AoA of 15° in Figure 3.

© ICMERE2011

Based as the Pressure contours seen in Figure 3 it is clear that the flow is modelled very differently and has very different characteristics. For the 1.5 million node mesh it is seen that the distribution of forces over the wing is very uneven and unclear. This would mean little confidence could be placed in this model. As the mesh is refined it can also be see that the flow characteristics become more defined and accurate. In addition to this increase in accuracy as the mesh was refined there was also corresponding increase in the Y+ values associated with each model. This results in a smoother more accurate mesh that is better capable of accurate modelling the flow characteristics over the configuration.

Though based on previously completed experimental flow visualisations it was seen that even the most refined model did not capture all of the flow characteristics over the configuration. These findings indicated that at 15° AoA there should be the beginning of a dual vortex formation occurring, though this was not seen in the CFD simulations. As a result a further refined model was developed with a concentration on refinements along the leading edge of the configuration. This model consisted of 22.5 million nodes and as a result could represent the dual vortex formation. The leading edge refinement can be seen in Figure 4. And the improved flow visualisation can be seen in Figure 3.

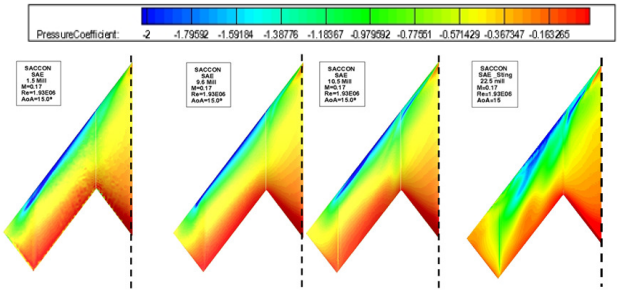

Fig. 3: Surface Contour Plots at 15° AoA, Comparing Mesh Refinement from 1.5 Mill to 22.5 Mill

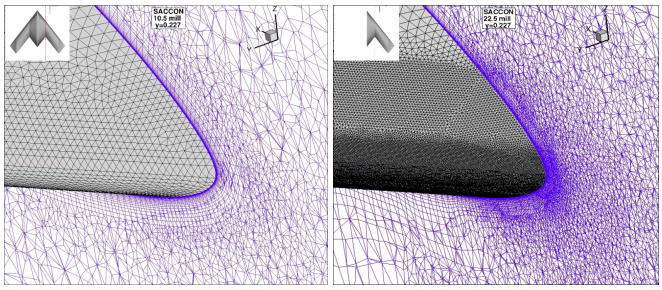

Fig. 4: Comparison of Leading Edge Refinement between 10.5 and 22.5 Million Node Meshes

Additionally it should be noted that a 22.5 million node mesh was developed with the pure purpose of improving the accuracy of low AoA results. This means that the mesh refinement was focused on leading edge and surface refinements. Based on the mesh refinement studies it was deemed valid to say that the 10.5million node mesh could be used in confidence for further testing with the knowledge that it will represent the flow characteristics accurately. Though it is recommended that for more accurate results or for any final conclusions, the more refined 22.5 million node model should be used. Additionally based on these results it was noted that the pitching moment coefficient was a good representation regarding the quality of the CFD results.

5.2 Sensitivity of Turbulence Models

When analysing the flow over the configuration, it is vital to determine the sensitivity of the results due to the turbulence models. The reason for this is that each turbulence model is developed for different applications and each has their own capabilities and drawbacks. If an incorrect model is chosen the quality and accuracy of the flow results will be degraded. Due to this it is important to select a range of turbulence models that are assumed to be appropriate and determine a sensitivity analysis to conclude which is most suitable for the particular configuration. It is important to note that some turbulence models that are expected to be of greater accuracy were not used. This includes such models as the Detached Eddy Simulation. The reason being, that this model would increase the accuracy of the results, though the corresponding computational time increase would be more than what is feasible for the scope of this paper. In the scope of this work the turbulence models that were looked at in greater detail were the SAE and k-ω models with an additional consideration of the LEA and SST turbulence models.

Extensive studies were done regarding the SAE and k-ω models. These two models were compared using the force and moment graphs, surface contour plots and pressure coefficient graphs. All three methods of testing were used to ensure a clear understanding between the accuracy and capabilities of the difference turbulence models. This process was then done again for the LEA and SST turbulence models. These tests were done at a range of AoA to ensure a consistent trend was seen. A representation of these tests can be seen in the pitching moment graphs in Figure 5

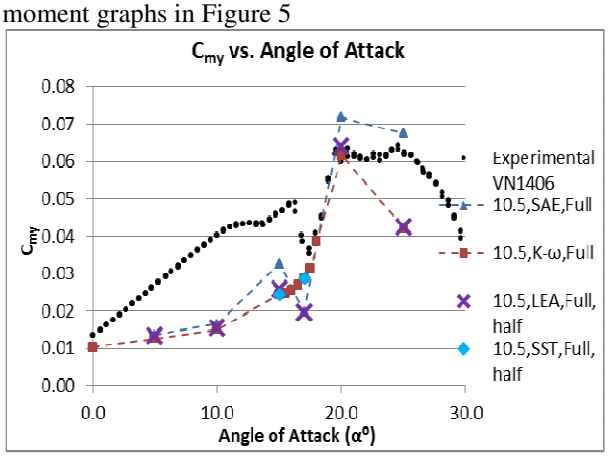

Fig. 5: Test VN 1406, SAE, k-ω, LEA and SST results C_{my} vs. Angle of Attack

Based on the comparisons seen in all of the turbulence models it was seen that the SAE model had the most consistent results. It was able to more accurately represent the flow phenomena than the other models as in models such as the k-ω model key flow phonemes such as the pitching moment dip at 17° were no represented. Also, as it is only a single equation model while the others are two equations, it is much simpler and as a result, the simulation runs much faster. This is beneficial as a large range of tests are desirable so a reduction in computation time means more tests can be made. Based

© ICMERE2011

on these results, the rest of the tests in this paper will be based on the SAE turbulence model. It is believed that although these results are still not ideal, this model is the closest, so should be the easiest to improve with further refinements.

5.3 Influence of Configuration Changes

When analysing the flow over the configuration it was noted that more than one layout for the model can be used. The two main alternatives that were looked at were the possibilities of using a half model configuration, and the effects of the wind tunnel sting attachment. The purpose of testing a half model is to prove the results for the full and half model are the same. If this is true, then it is possible to make a flow analysis with greater mesh refinements over the half model. The advantage of the half model is it is faster to solve, though also it allows for additional refinement. The purpose of testing the effects of the sting attachment is that it is unknown if the sting is a cause of some of the errors in the flow, by comparing this, it will determine if a sting should be used for further studies to achieve accurate results.

To compare the full and half model, several angles were reviewed, looking at, the force and moment graphs as well as the surface contour plots. Based on these results it was seen that all of the features of the flow was the same for both the full and half model. Due to their similarity the data was not shown in this paper.

The next test in configuration changes was to determine the effects the wind tunnel sting attachment would have on the flow phenomena. Tests were performed on a range of AoA between 10º and 20º. When review these results it was seen that in general the effect of the sting attachment was to translate the pitching moment results upwards. As the results for pitching moment coefficients were generally under predicting the results, the upwards shift is beneficial to the results. Based on these findings it is recommended that for final simulations the sting attachment should be included in the model configuration. The pitching moment coefficient graph can be seen in Figure 6.

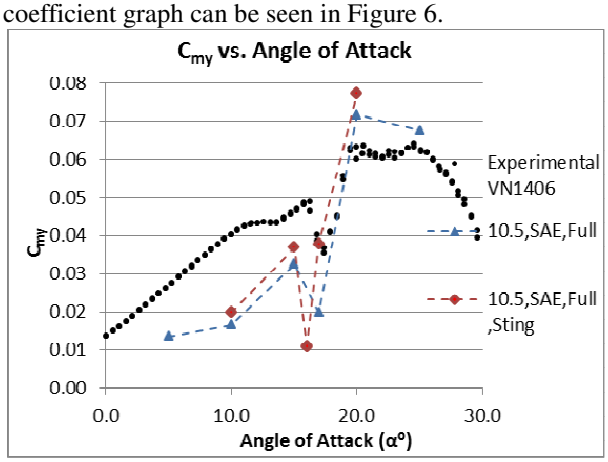

Fig. 6: Test VN 1406, SAE, With and Without Sting, C_{my} vs. Angle of Attack

5.4 Influence of Discretisation Parameters

When simulations are run for the configuration there are a range of parameters that are within the code that regulate how the calculation process is determined. Some of these determine the characteristics of the flow, and others effect how the calculations are made. Two of the parameters that were reviewed in the scope of this paper are Preconditioning and the Dissipation parameters. Both of these will affect the results of the flow simulations in different ways. Precondition alters the calculation assumptions regarding incompressible flow which is required due to the low speeds of the simulation. While the Dissipation parameters refer to the degradation of the intensity in vortical flow.

Based on the results seen in the pitching moment graph it was noted that at low AoA the changes in the pitching moment coefficients were negligible. Then when reviewing the results at higher AoA it was seen the two of the tests had noticeable effects on the results. With these inputs it was seen that the pitching moment values that were previously over predicting the experimental data were translated back down onto the experimental results. The results of these tests are not shown due to space limitations. Though there findings were used for the final simulations.

5.5 Finalised Simulation

Both of the discretisation parameters were investigated separately and found to affect their flow in different ways. The next step was to try and find the optimum parameters to gather the most accurate model. To attempt this, simulations with both the precondition and dissipations values decided on previously will be used together. In addition to these parameters, to try and improve the overall quality of the results, factors seen to be beneficial to the results previously were also implemented. Because of this a mesh of 22.5 million nodes was used on the half model configuration. In addition to this the sting attachment was also used. The goal of this was to implement the lessons seen previously together to gain the most accurate results possible. To see the effect of these concepts being assembled, the force and moment graphs were put together to compare the changes. From these results the pitching moment coefficient values can be seen in Figure 7.

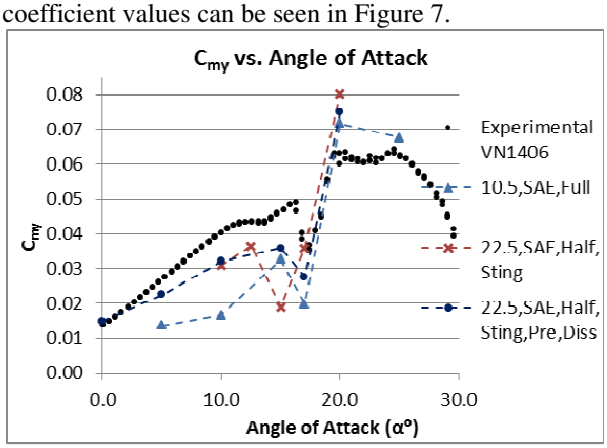

Fig. 7: Test VN 1406, SAE, Standard, Sting and Dissipation + Preconditioning, C_{my} vs. Angle of Attack

When reviewing the pitching moment coefficients it was seen for low AoA, the value translated up greatly, much closer to the experimental results. As the AoA increased it was noted that the values of the pitching moment coefficient dipped further below the experimental results. To determine the reasons for this, additional AoA simulations were run. With these results it became clear that the pitching moment dip was now

© ICMERE2011

occurring earlier then seen previously. This concept appears constant for the rest of the AoA. Based on these results it appears that the mesh refinement, half model and sting attachment together translate the entire pitching moment graph to the left. This means that simulation is predicting the flow phenomena before it should have occurred.

To further explain the changes in flow characteristics of the model, pressure surface contour plots and contour plots with stream lines were created. Though when reviewing the contour plots it became apparent there were little difference between the improved model and the slandered model configuration. To try and help explain the flow better, results for the pressure coefficient graphs were developed. These were done at the pressure tap locations that lie on the 62% span line, running perpendicular to the leading edge, the 45% and 70% chord lines and the 26% span line along the length of the configuration. The graphs lie in this order respectively grouped by their corresponding AoA. Through the use of pressure contour plots a greater representation of the flow phenomena could be seen. These graphs were able to clearly represent the formations and dispersion of the vortices over the configuration. Through the use of these graphs it became apparent that in general the half model with sting, preconditioning and dissipation was capable of more accurately representing the flow characteristics. Despite some deviations of the results at higher AoA, the improvements for lower AoA were more noticeable and in general improved the overall quality of the results. The flow characteristics can also be seen visually in the surface contour plots in Figure 8 for this final configuration choice

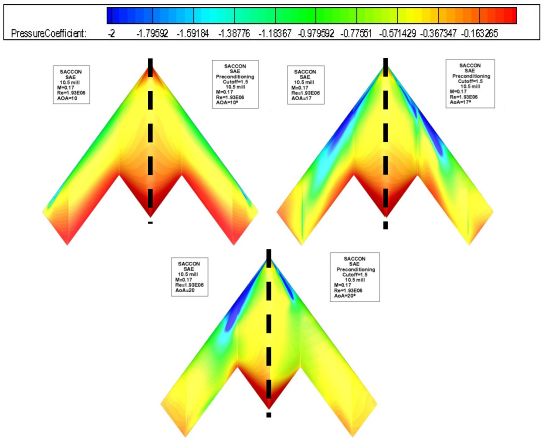

Fig. 8: Surface Contour Plots of Model with Precondition, Dissipation and Sting

6. CONCLUSIONS

Based on the findings from the CFD testing that was performed in the scope of this work, a final simulation was created utilising all of the beneficial simulations factors that were seen. This meant running simulations on the 22.5 million node half model, with the sting attachment, preconditioning and dissipation parameters.

It was noted that this model was quite capable of providing acceptably accurate results. Though in order to use the results in good confidence, only the low level AoA range should be used - this is between 0º and 15º.

With the current results found in this work it was seen that with the appropriate mesh refinement and flow parameters, the TAU code is capable of representing the force and moment coefficient results to an appropriate level of accuracy. This means that this simulation could be run in confidence and be sure that the results would describe the characteristics of the flow for these values.

7. ACKOWLEDGEMENT

The author is highly grateful to Dr. Stephan Hitzel and Dr Herbert Rieger, from CASSIDIAN – Air systems for his assistance and support with the organisation and preparation of this work. As well as for their time and effort spent in ensuring it was produced to a high standard

7. REFERENCES

[1] Gursul, I., Gordinier, R., and Visbal, M. "*Unsteady Aerodynamics of Nonslender Delta Wings*",s.l. : Elsevier Ltd., 2005.

[2] Century of Flight, "Development of Aviation Technology - Delta Wings", 2010, [cited January.2011] Available from: http://www.century-of-flight.net

[3] Surruno, "Pakistan Defence - Wing Planforms" , 2009, [cited January.2011] Available from: http://www.defence.pk/forums/india-defence/4346-lca-news-discussions-316.html

[4] Visbal, M.R., "Computational and Physical Aspects of Vortex Breakdown on Delta Wings", Reno, NV:s.n., 9th -12th January 1995. 33rd AIAA Aerospace Sciences Meeting and Exihibit

[5] Gursul, I., "Recent Developments in Delta Wing Aerodynmaics", The Aeronatical Journal, September 2004.

[6] Frink, N.T., "Strategy for Dynamic CFD Simulations on SACCON Configuration," AIAA Paper 2010-4559, June.2010.

[7] Vicroy, D.D., Loeser, T.D., Schütte, A., "SACCON Forced Oscillation Tests at DNW-NWB and NASA Langley 14X22-foot Tunnel", AIAA Paper 2010-4394, June.2010

[8] Schütte, A., Hummel, D., Hitzel, S.M., "Numerical and experimental analyses of the vortical flow around the SACCON configuration" AIAA Paper 2010-4690, July, 2010.

[9] Hübner, A.R., "Experimental and Numerical Investigations of Unsteady Aerodynamic Derivatives for Transport Aircraft Configurations" AIAA Paper 2007-1076, January, 2007.

8. NOMENCLATURE

Symbol	Meaning	Unit
C_D	Coefficient of Drag	-
C_L	Coefficient of Lift	-
C_{my}	Coefficient of Pitching Moment	-
C_p	Coefficient of Pressure	-

© ICMERE2011